The Multi-Messenger Astrophysics of the Galactic Centre
Proceedings IAU Symposium No. 322, 2016
R.M. Crocker, S.N. Longmore & G.V. Bicknell, eds.

doi:10.1017/S1743921316012278

How hot is the molecular gas in the Galactic Center?

Katharina Immer[1], Jens Kauffmann[2], Thushara Pillai[2], Adam Ginsburg[1] and Karl M. Menten[2]

[1]European Southern Observatory
Karl-Schwarzschild-Strasse 2, 85748 Garching bei München, Germany
email: kimmer@eso.org

[2]Max-Planck-Institut für Radioastronomie
Auf dem Hügel 69, 53121 Bonn, Germany

Abstract. The molecular clouds in the Central Molecular Zone of our Galaxy (CMZ; inner ∼200 pc) show systematically higher gas than dust temperatures (>50 K vs <30 K) in recent H_2CO line and dust continuum surveys. This discrepancy is puzzling since gas and dust temperatures should become equal over short times at the high densities observed in these clouds. In deep $H_2CO(3-2)$ and $(4-3)$ observations of seven clouds in the CMZ, we detected not only large temperature differences between the clouds but also large gradients within the clouds. Comparing the temperatures and the main H_2CO lines at 218 and 291 GHz, we found a positive correlation between those two parameters, indicating that turbulence plays an important role in the heating of the gas. As a follow-up, we mapped the temperature tracers CH_3CCH and CH_3CN in these seven clouds to derive multiple temperature estimates and test the accuracy of high gas temperatures.

Keywords. Galaxy: center, ISM: molecules, ISM: structure, ISM: clouds, Submillimeter: ISM

1. Motivation

In the Central Molecular Zone (CMZ, inner ∼200 pc of our Galaxy), we can study star formation under extreme conditions. Here, the velocity dispersion, gas temperatures, magnetic field strengths, pressure, etc. are much higher than in the Galactic disk (Morris & Serabyn 1996). Recent CMZ surveys have shown that the gas temperatures (> 50 K; Güsten *et al.* 1981; Hüttemeister *et al.* 1993; Ao *et al.* 2013; Mills & Morris 2013; Ott *et al.* 2014; Ginsburg *et al.* 2016; Immer *et al.* 2016) in the Galactic center clouds are much higher than the dust temperatures (< 20 K; Lis *et al.* 1999; Molinari *et al.* 2011).

While many previous gas temperature measurements are based on observations of the ammonia molecule which traces low-density gas ($n \sim 10^3$ cm^{-3}), we used the H_2CO thermometer for our gas temperature study of CMZ clouds. H_2CO is a slightly asymmetric rotor molecule. It has two different species (i.e. ortho and para) whose differences in the level populations are due to collisions. Comparing the relative intensities of para-H_2CO lines within the same K_a ladder gives estimates of the gas temperature (Mangum & Wootten 1993). Since the transitions of the K_a ladders are close in frequency, they can be observed within one spectrum, making them calibration-independent. These gas temperature measurements and the further results are published in Immer *et al.* (2016)

To test if the H_2CO temperatures are representative of the bulk of the CMZ gas or if there is a selection bias towards warmer temperatures or higher densities in our H_2CO results, we observed the temperature tracers CH_3CN and CH_3CCH towards the same sample of clouds. Both molecules have transitions that are sensitive to very hot gas if there is any. The analysis of this data is ongoing (Immer *et al.*, in prep.).

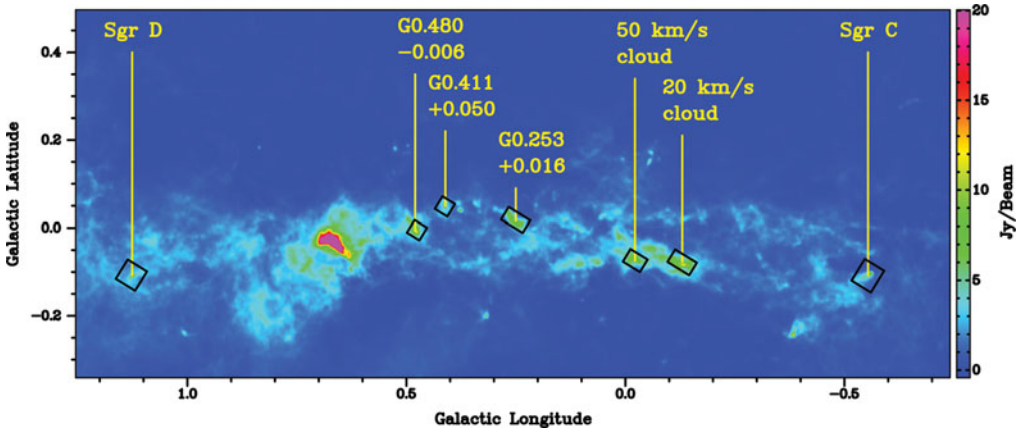

Figure 1. 870 μm emission of the CMZ from the ATLASGAL survey (Schuller *et al.* 2009). The targets of our temperature study are marked. The boxes show the sizes of the observed OTF maps. Figure adopted from Immer *et al.* 2016a.

2. Observations

In 2012 and 2014, we mapped the $H_2CO(3-2)$ and $(4-3)$ multiplets at 218 and 291 GHz with the Swedish Heterodyne Facility Instrument (SHeFI, Vassilev *et al.* 2008) and First Light APEX Submillimeter Heterodyne (FLASH) receiver (Heyminck *et al.* 2006; Klein *et al.* 2014) at the Atacama Pathfinder EXperiment (APEX†; Güsten *et al.* 2006) telescope towards five and seven CMZ clouds (Fig. 1), respectively. In 2015, we mapped the same seven clouds in the CH_3CN/CH_3CCH ladders at 165/170 GHz and 202/205 GHz with Band 5 of the Swedish-ESO PI receiver at APEX (SEPIA; Immer *et al.* 2016b). The data are smoothed to a velocity resolution of 1 km s^{-1}. The beam sizes at 170, 205, 218, and 291 GHz are 37″, 31″, 30″, and 24″, respectively.

3. H_2CO gas temperature measurements

To measure the gas temperatures in our clouds, we produced integrated intensity maps of the transitions $H_2CO(3_{2,1}-2_{2,0})$, $H_2CO(3_{0,3}-2_{0,2})$, $H_2CO(4_{2,2}-3_{2,1})$, and $H_2CO(4_{0,4}-3_{0,3})$ for all velocity components of our targets (Fig. 2 for the 8−14 km s^{-1} velocity component of the 20 km/s cloud) . Then, for each pixel in these maps, we determined the ratios $R_{321} = \frac{\int I_{H_2CO(3_{2,1}-2_{2,0})}\, d\mathrm{V}}{\int I_{H_2CO(3_{0,3}-2_{0,2})}\, d\mathrm{V}}$ and $R_{422} = \frac{\int I_{H_2CO(4_{2,2}-3_{2,1})}\, d\mathrm{V}}{\int I_{H_2CO(4_{0,4}-3_{0,3})}\, d\mathrm{V}}$, yielding integrated intensity ratio maps (see Fig. 3, left, for the 8−14 km s^{-1} velocity component of the 20 km/s cloud). We used RADEX (van der Tak *et al.* 2007) to create model intensities for the para-H_2CO lines from which we then calculated the same ratios R_{321} and R_{422}. In the end, we yield functions which give estimates of the kinetic gas temperatures for given R_{321} and R_{422}. Combining our integrated intensity ratio maps with the radiative transfer models, we yield two independent gas temperature maps for each velocity component of each target (see Fig. 3, right, for the 8−14 km s^{-1} velocity component of the 20 km/s cloud; for more details of this analysis, please see Immer *et al.* 2016a).

Consistent with previous surveys, we measure high gas temperatures above 50 K in all our sources. In the temperature maps, we detect clear temperature gradients. This is an indication that heating mechanisms that act uniformly on the bulk of the molecular

† APEX is a collaboration between the Max-Planck-Institut für Radioastronomie, the European Southern Observatory, and the Onsala Space Observatory.

https://doi.org/10.1017/S1743921316012278 Published online by Cambridge University Press

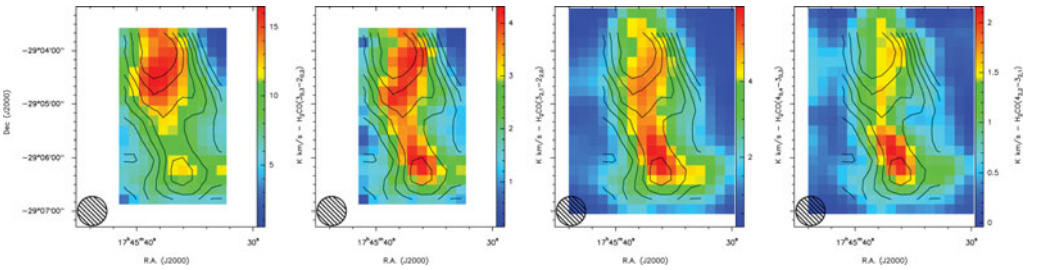

Figure 2. H_2CO integrated intensity maps (from left to right: $H_2CO(3_{0,3}-2_{0,2})$, $H_2CO(3_{2,1}-2_{2,0})$, $H2CO(4_{0,4}-3_{0,3})$, and $H_2CO(4_{2,2}-3_{2,1})$) for the 8−14 km s^{-1} component of the 20 km/s cloud. The contours show the moment 0 map of the $H_2CO(3_{0,3}-2_{0,2})$ transition, produced over the whole velocity range of the source (levels: 30%−90% of the maximum in steps of 10%). The circle in the lower left corner shows the 33″ beam. Figure adopted from Immer *et al.* 2016a.

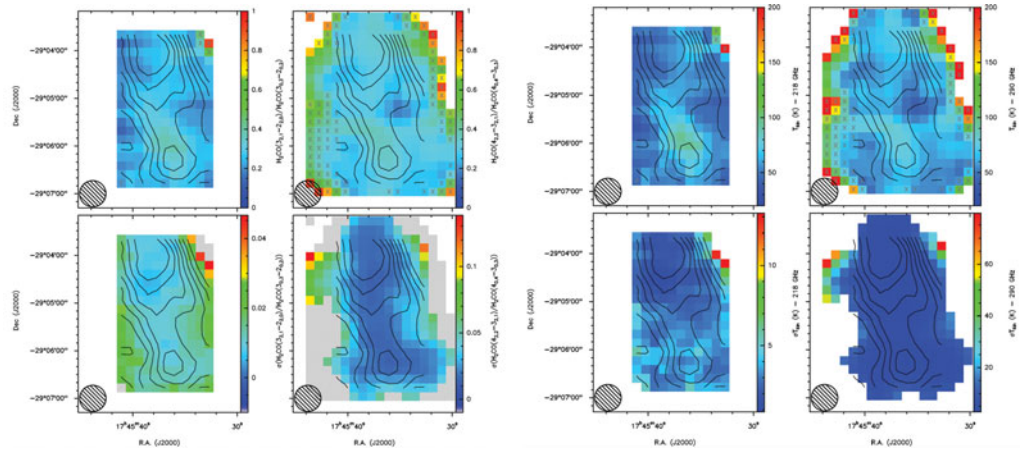

Figure 3. Left: H_2CO ratio (upper panels) and uncertainty maps (lower panels) (left: R_{321}, right: R_{422}). Right: H_2CO temperature (upper panels) and uncertainty maps (lower panels), derived from the 218 GHz (left) and 291 GHz data (right). Contours and beam as in Fig. 2. Figure adopted from Immer *et al.* 2016a.

gas cannot play an important role in the heating of the gas. We found a clear positive correlation between the line widths of the main H_2CO lines at 218 and 291 GHz and the measured temperatures which points towards turbulence being one of the main heating agents of the gas.

4. CH_3CN/CH_3CCH gas temperature measurements

The $CH_3CN(9-8)$ and $(11-10)$ ladders at 165 and 202 GHz, respectively, and the $CH_3CCH(10-9)$ and $(12-11)$ ladders at 170 and 205 GHz, respectively, are detected towards all our sources. In some sources, we even detect the $CH_3CN(12-11)$ transitions at 220 GHz which were observed in the same band as the H_2CO 218 GHz transitions. In Fig. 4, we show the CH_3CN ladder at 165 GHz and the rotational temperature diagram of the 36−42 km s^{-1} component of G0.253+0.016 towards the temperature peak of the source. Five, four and four CH_3CN transitions are detected at 165, 202, and 221 GHz, respectively, and fitted. The rotational temperature diagram shows that a low and a high temperature component is necessary to fit the data. In the future, we will model the detected lines in each pixel of the maps with the XCLASS software (Möller *et al.* 2015) by

https://doi.org/10.1017/S1743921316012278 Published online by Cambridge University Press

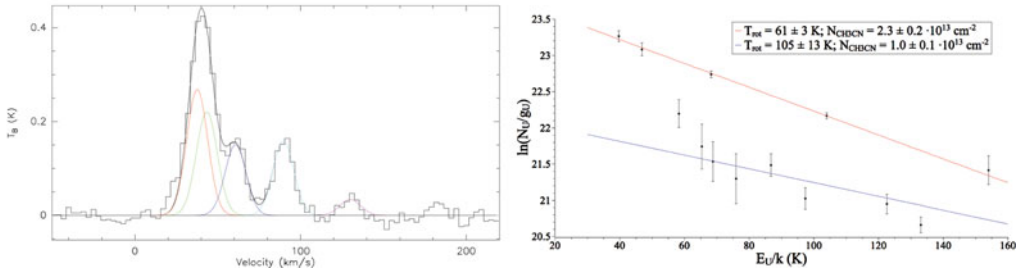

Figure 4. Left: Spectrum of $CH_3CN(9-8)$ at 165 GHz towards the temperature peak of G0.253+0.016. Five transitions are detected and fitted. Right: Rotational temperature diagram towards the same position from all detected CH_3CN transitions at 165, 202, and 220 GHz. A low and a high temperature component are necessary to fit the data.

solving the radiative transfer equation. Thus, we will produce independent temperature maps for CH_3CN and CH_3CCH for all velocity components of all our sources.

References

Ao, Y., Henkel, C., Menten, K. M., *et al.* 2013, *A&A*, 550, A135
Ginsburg, A., Henkel, C., Ao, Y., *et al.* 2016, *A&A*, 586, A50
Güsten, R., Nyman, L. Å., Schilke, P., *et al.* 2006, *A&A*, 454, L13
Güsten, R., Walmsley, C. M., & Pauls, T. 1981, *A&A*, 103, 197
Heyminck, S., Kasemann, C., Güsten, R., de Lange, G., & Graf, U. U. 2006, *A&A*, 454, L21
Hüttemeister, S., Wilson, T. L., Bania, T. M., & Martin-Pintado, J. 1993, *A&A*, 280, 255
Immer, K., Kauffmann, J., Pillai, T., *et al.* 2016, ArXiv e-prints (1607.03535)
Immer, K., Belitsky, V., Olberg, M., *et al.* 2016, *The Messenger*, 165, 13
Klein, T., Ciechanowicz, M., Leinz, C., *et al.* 2014, IEEE Transactions on Terahertz Science and Technology, 4, 588
Lis, D. C., Li, Y., Dowell, C. D., & Menten, K. M. 1999, in ESA Special Publication, Vol. 427, The Universe as Seen by ISO, ed. P. Cox & M. Kessler, 627
Mangum, J. G. & Wootten, A. 1993, *ApJS*, 89, 123
Mills, E. A. C. & Morris, M. R. 2013, *ApJ*, 772, 105
Möller, T., Endres, C., & Schilke, P., 2015, ArXiv e-prints (1508.04114)
Molinari, S., Bally, J., Noriega-Crespo, A., *et al.* 2011, *ApJ*, 735, L33
Morris, M. & Serabyn, E. 1996, *ARAA*, 34, 645
Ott, J., Weiß, A., Staveley-Smith, L., Henkel, C., & Meier, D. S. 2014, *ApJ*, 785, 55
Schuller, F., Menten, K. M., Contreras, Y., *et al.* 2009, *A&A*, 504, 415
van der Tak, F. F. S., Black, J. H., Schöier, F. L., Jansen, D. J., & van Dishoeck, E. F. 2007, *A&A*, 468, 627
Vassilev, V., Meledin, D., Lapkin, I., *et al.* 2008, *A&A*, 490, 1157

https://doi.org/10.1017/S1743921316012278 Published online by Cambridge University Press